Electronic structure of BAs and boride III-V alloys

Gus L. W. Hart and Alex Zunger
National Renewable Energy Laboratory, Golden, Colorado 80401
Received 16 June 2000)

Boron arsenide, the typically ignored member of the Group-III–V arsenide series BAs-AlAs-GaAs-InAs is found to resemble silicon electronically: its Γ conduction-band minimum is *p*-like (Γ_{15}), not *s*-like (Γ_{1c}), it has an X_{1c}-like indirect band gap, and its bond charge is distributed almost equally on the two atoms in the unit cell, exhibiting nearly perfect covalency. The reasons for these are tracked down to the anomalously low atomic *p* orbital energy in the boron and to the unusually strong *b* is larger than the difference of the band)Tj /F6 1 Tf -41.4582 -1.2778 TD (~)Tj /F11 1 Tf 0.333 0 TD (ii)Tj /F6 1

gaps of the constituents e.g., ZnS-ZnTe; GaAs-GaN). In this case addition of small amounts of the wide gap components acts to initially lower the band gap of the small gap component. For example, one can achieve the technologically desired 1-eV gap if one adds nitrogen to GaAs or to InGaAs.

When boron is substituted into GaAs, it can go to either a gallium site or an arsenic site. Normally boron prefers isovalent substitution on the gallium site,[1–3] which is the case we study here. In the other case when boron goes to the arsenic site a boron ‘‘antisite’’ defect), the boron acts as an acceptor and this antisite defect has been the subject of numerous studies.[4–8] Growth conditions determine whether boron goes to the gallium site as an isovalent substitution or to the arsenic site as an acceptor. For example, B_{As} antisite defects are known to occur in Ga-rich samples of GaAs grown by the liquid encapsulated Czochralski method, but for GaAs crystals taken from stoichiometric or As-rich melts, electrically active boron or boron complexes are not found,[9] indicating that the boron atoms have substituted isovalently to the gallium sites. Not as much is known about the *epitaxial* growth conditions under which isovalent or antisite boron incorporation occurs. It is reasonable to suppose that B_{As} antisite defects will be more likely under Ga-rich conditions and that As-rich growth conditions will lead to isovalent boron incorporation, similar to the case for LEC-grown GaAs. In this paper, we focus on isovalent BGaAs alloys where boron occupies gallium sites.

In this paper we will explore BAs as an alternative toGaN as a wi

anomalous as the very large and composition dependent) bowing in $GaAs_{1-x}N_x$?

iv) Will cation substitution by boron lead to unusual wave function localization effects found to exist for anion substitition by nitrogen?[27–29]

Two features of boron make boride semiconductors fundamentally different from common Group-III–V or Group-II–VI semiconductors. The first is that, like nitrogen, boron is in the first row of the Periodic Table and has deep *p* orbitals and a small atomic size. The second feature is, unlike nitrogen, boron has a low electronegativity. This leads to highly covalent compounds, unlike nitride semiconductors, which have a strong ionic character. This paper examines i) zincblende BAs and its place in the Group-III–As family of semiconductors and ii) boron substitution of gallium in GaAs, including alloy bowing, band offsets, and mixing enthalpies. Our main findings are:

Zincblende BAs: Surprisingly, we find that, electronically, BAs resembles silicon rather than other Group-III–V semiconductors. Similar to silicon and in contrast to most Group-III–V's, the lowest Brillouin-zone center conduction band of BAs has *p* symmetry (Γ_{15c}) rather than *s* symmetry (Γ_{1c}), and, like silicon, its total valence charge density shows almost symmetric distribution of charge around the two atoms in the unit cell. The reasons for the siliconlike conduction-band ordering in BAs are: i) the small repulsion of the bonding and antibonding *p* states due to the low *p* orbital energy of boron, as well as the unusual hybridization of both cation and anion *p* states at the VBM, and ii) the repulsion of the cation and anion *s* states that is much stronger in BAs than in AlAs, GaAs, and InAs. As a result of the *p*-*p* hybridization covalent bonding) mentioned in i), we also find that the valence-band offset of BAs relative to other members of the Group-III–As family is unusually high.

BAs–GaAs alloys: i) The band-gap bowing is relatively small ($\sim$3.5 eV) and composition independent, in stark contrast to GaN-GaAs alloys. Because of this small bowing, the addition of BAs to GaAs *increases* the gap, thus, unlike nitrogen, addition of boron into GaAs or InGaAs will not lead to the desired 1 eV material. ii) The lower energy conduction-band states are ''semilocalized'' states around the boron atoms, e.g., the conduction-band maximum CBM) is strongly localized near the boron but extended at longer distances while the VBM is completely delocalized. iii) The bulk mixing enthalpy of BAs in GaAs is much lower than that of GaN in GaAs, indicating that the bulk solubility of boron in Group-III–V compounds may be higher than that of nitrogen and thus higher composition ranges may be possible with the boride alloys. These findings indicate that boride Group-III–V alloys provide new opportunities in band-gap engineering.

II. METHODS OF CALCULATION

A. The LAPW calculations

We used density-functional theory within the local-density approximation LDA),[30] as implemented by the full-potential linearized-augmented-plane waves LAPW) method[31,32] WIEN97 implementation[33]). The exchange-correlation potential of Perdew and Wang was used.[34] In the calculations with less than 32 atoms, the plane-wave kinetic-energy cutoff for the expansion in the interstitial region was 16 Ry approximately 130 basis functions per atom). The muffin-tin MT) radii were 1.65 bohr for boron and 2.2 bohr for arsenic, aluminum, gallium, and indium. In the large supercell calculations 32 or more atoms), a slightly smaller plane-wave kinetic-energy cutoff of 13 Ry approximately 120 basis functions per atom) and a larger boron MT radius of 1.8 bohr 2.1 for arsenic, aluminum, gallium, and indium) was used to ease the computational burden of the larger cells. Our convergence studies indicate that the error in the individual eigenstates is less than 5 meV for the valence and lower-conduction bands. The calculations were run until the variation in the total energy between several self-consistency cycles was $<10^{-5}$ Ry. The experimental lattice constants were used in all the calculations of the individual compounds. The experimental lattice constants are 4.777, 5.660, 5.653, and 6.058 Å for BAs, AlAs, GaAs, and InAs, respectively.

The *k*-point mesh used in the calculation of the simple binary compounds zincblende BAs, AlAs, GaAs, and InAs) was a $4\times4\times4$ mesh of Monkhorst and Pack special points [10 points in the irreducible wedge of the Brillouin zone BZ)].[35] The superlattice calculations for the valence-band offsets as well as the supercell calculations for the alloy studies used *k*-point meshes equivalent[36] to the $4\times4\times4$ mesh used in the calculation of the simple zincblende binary compounds. Using equivalent *k*-point meshes is particularly important for calculations such as enthalpies of formation in order to eliminate uncertainties due to the statistical errors of different *k*-point meshes. Thus, one can use much smaller *k*-point meshes to achieve the required accuracies than would otherwise be necessary.

B. Partial DOS, band characters, and valence charge density

It is useful to analyze the orbital character of different states. The band character or orbital population) $Q_l^{(\ )}(\ ,\mathbf{k})$ is the lth angular momentum component of the charge due to wave function $(\ ,\mathbf{k})$ enclosed in a sphere $_{\mathrm{MT}}$ of radius $R_{\mathrm{MT}}^{(\ )}$ about atom :

$$Q_l^{(\ )}\ ,\mathbf{k})=\int_{\mathrm{MT}}|\hat{P}_l\ \ ,\mathbf{k},\mathbf{r})|^2 d\mathbf{r}, \qquad 1)$$

where $\hat{P}_l$ is an angular momemtum projection operator with origin at site . Because the interstitial region outside the

Valence charge densities: The charge density is constructed from the highest N_B occupied bands as

$$, _{\mathrm{val}}\ \mathbf{r}) = \sum_{n=1}^{N_B} \int_{\mathrm{BZ}}$$

of accomplishing this is to increase the number of k points in all three systems until convergence is obtained. The disadvantage of this approach is that it requires *absolute* k-point convergence for A and B, and separately for A_pB_q. A better approach is to take advantage of *relative* k-point convergence.[36] The idea is to sample the Brillouin zone *equivalently* for A, B and A_pB_q. This could be done by considering A_pA_q, B_pB_q, and A_pB_q as isostructural solids and sampling the Brillouin zone of each equally. Then, any relative k-point sampling error cancels out. This is called the *method of equivalent k points*.[36] In practice, one does not have to calculate A_pA_q and B_pB_q but instead can calculate A and B in their primitive unit cells using suitably folded-in k points. Equivalent k points for the unit cells in this paper are given in Table II.

E. Choice of supercells

The calculations of ΔH [Eq. 9)] and b [Eq. 10)] require supercells. We use $B_1Ga_7As_8$, $B_1Ga_{15}As_{16}$, $B_1Ga_{31}As_{32}$, and $B_2Ga_{30}As_{32}$. The lattice vectors defining the supercells are given in Table II. The SQS16 supercell is a ''special quasirandom structure''—a periodic structure with a rather small unit cell whose lattice sites are occupied by A and B atoms so as to mimic the atom-atom correlation functions of much larger $A_{1-x}B_x$ supercells with random occupations.[39]

In the calculations for the band-gap bowing of $B_xGa_{1-x}As$ alloys, 64 atom, simple-cubic unit cells were used for both the 3% and 6% boron alloys. In the case of the 3% alloy, there is one boron atom in the supercell, but for the 6% alloy, there are two boron atoms in the supercell. For this case, the band-gap was determined by taking the weighted average of the gaps for the 5 symmetrically inequivalent configurations given in Table III) of two boron atoms in the 64-atom supercell. These five pairs are the first through fourth neighbor pairs in an fcc lattice, as well as the sixth neighbor. In the 64-atom cell, the fifth fcc neighbor is equivalent to the first.) Using the same 64-atom unit cell for the alloys in the bowing calculations eliminated band-gap differences that can occur due to the k-point folding relations

TABLE II. Definition of the supercells used in this study and equivalent k points. Lattice vectors are given in units of a_0 and equivalent k points are given as fractions of the reciprocal lattice vectors.

System	Lattice vectors	Equivalent k points	Relative weight
AC, BC zincblende	1/2, 1/2, 0)	0, 0, 1/8)	1
	1/2, 0, 1/2)	0, 0, 3/8)	1
	0, 1/2, 1/2)	0, 1/8, 3/4)	3
		0, 1/8, 1/4)	3
		0, 1/8, 1/2)	3
		0, 1/4, 5/8)	3
		1/8, 1/4, 1/2)	6
		0, 1/4, 3/8)	3
		0, 3/8, 1/2)	3
		1/8, 3/8, 5/8)	6
$(AC)_1/(BC)_1$ 100			

the band gap of BAs is indirect; the CBM is along the Δ line between the Γ and X points—at approximately $0.82(1,0,0)2\pi/a$. An unusual feature of the band structure is the character of the CBM at Γ. In BAs, the CBM is the *p*-like Γ_{7c} state (Γ_{15c} if spin-orbit interaction not included). Only the semiconductors silicon and BP share this feature. In most semiconductors, the lowest state at Γ is the singly degenerate *s*-like state. The origins of this feature of the BAs band structure can be understood in the context of the tight-binding model of Harrison.[43] According to this model, the bonding (Γ_{15v}) and antibonding (Γ_{15c}) *p* states at Γ are given by

$$E(\Gamma_{15}) = \frac{E_p^c + E_p^a}{2} \pm \sqrt{\left(\frac{E_p^c - E_p^a}{2}\right)^2 + 4E_{pp})^2}, \qquad (11)$$

The large Γ_{1v}F

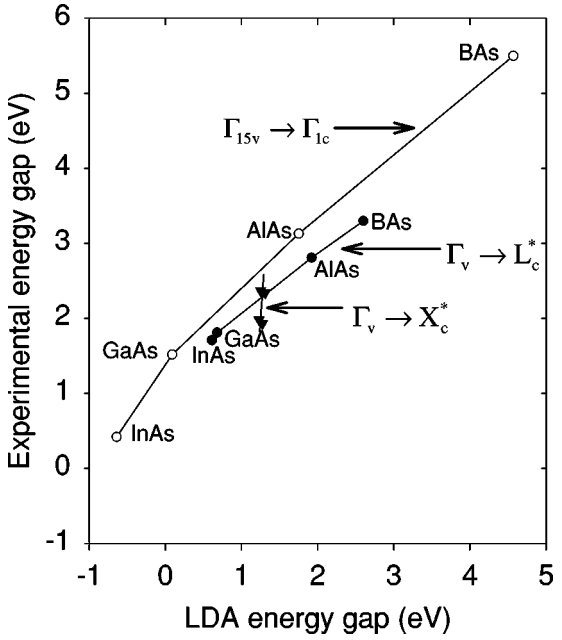

FIG. 7. Trends in the LDA vs experimental band-gaps of the Group-III-As family. For the $\Gamma_{15v} \rightarrow \Gamma_{1c}$ and the $\Gamma_{15v} \rightarrow L_c$ gaps, the errors are nearly constant. The LDA errors are $\sim 1-1.5$ eV and $\sim 0.7-1.1$ eV for the $\Gamma_{15v} \rightarrow \Gamma_{1c}$ and the $\Gamma_{15v} \rightarrow L_c$ gaps, respectively.

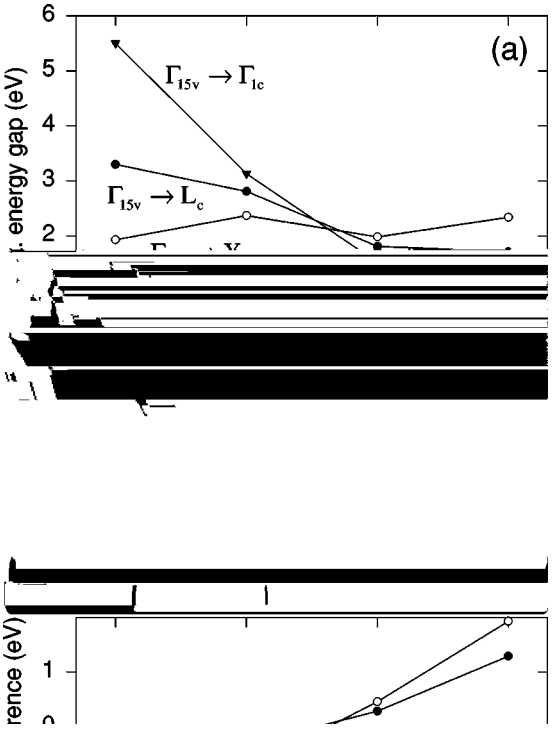

FIG. 8. Trends in the intervalley energy seperations of the Group-III-As family. Note the crossing of the $\Gamma_{15v} \rightarrow X_c$ gaps and the $\Gamma_{15v} \rightarrow \Gamma_{1c}$ gaps between AlAs and GaAs. Thus, GaAs and InAs are direct gap materials whereas BAs and AlAs are indirect X gap materials.

AlAs relative to BAs: Two effects increase the VBM of BAs relative to the VBM of AlAs. i) Because the unoccupied d states in BAs lie very high in energy relative to the VBM, the p-d repulsion effect that drives the VBM down in AlAs is weaker in BAs. ii) The more important effect is the unusual character of the VBM in BAs. In the rest of the Group-III-As family, the character of the VBM is primarily anion p-like, but in BAs the bonding is much more covalent and the VBM comes from both the anion and the cation Fig. 6). Since the cation p levels are higher in energy than the As p levels Fig. 1), any admixture of cation p character pulls the VBM up. These two effects, lack of p-d repulsion and strong hybridization of the cation p character into the VBM, account for the high VBM of BAs relative to AlAs.

GaAs relative to BAs: While the VBM of BAs and GaAs both lie above that of AlAs for the reasons given above, the VBM of BAs lies only slightly below that of GaAs despite the much smaller lattice constant ($\sim 17\%$ mismatch) and the lack of p-d repulsion. This is due to the unusual cation p hybridization into the VBM of BAs, which raises the VBM by several tenths of an eV.

Finally, we note that the transitivity among the band offsets of BAs/AlAs/GaAs is similar to other compounds where the lattice mismatches are not as large. By transitivity we mean that the band offset $\Delta E_v(A/C)$ between two compounds A and C is well approximated as the sum of the band offsets between compounds A and B and between compounds B and C, i.e.,

$$\Delta E_v \text{ GaAs/BAs}) \cong \Delta E_v \text{ BAs/AlAs}) + \Delta E_v \text{ AlAs/GaAs}). \quad 13)$$

In this case, ΔE_v(GaAs/BAs) calculated directly, yields 0.19 eV but ΔE_v(BAs/AlAs)$+\Delta E_v$(AlAs/GaAs) yields 0.12 eV, a nontransitivity difference of 0.07 eV.

V. BAs-GaAs ALLOYS

A. Bond lengths and bond angles in the alloys

Interest in BAs-GaAs alloys centers around the hope that boron will modify the GaAs band-gap similarly to nitrogen without the adverse effect[50] of introducing localized states that reduce carrier diffusion length. We know from the theory of Group-III–V alloys[29,51] that the optical properties are decided by both the atomic relaxation and by charge transfer. Thus, we first study the bond relaxation around a boron substitutional impurity.

The bond lengths and angles in the 110) plane of GaAs with $\sim 3\%$ boron substitution ($B_1Ga_{31}As_{32}$ supercell) are shown in Fig. 12. Bond lengths are shown as a percentage of the pure bulk GaAs bond length, except for the B-As bonds where the values indicate a percentage of the pure bulk BAs bond length. The numbers that lie between a triplet of atoms indicate the bond angle between the three atoms as a percentage of the ideal bond angle in the zincblende structure of 109.47°. The rectangle represents the supercell boundary. We note several observations:

i) Bond angles near boron increase by up to 5% from their ideal value. This helps accommodate the Ga-As and B-As alloy bonds hereafter R_{GaAs} and R_{BAs}, respectively) to keep the bond lengths close to their ideal values, R^0_{BAs} and R^0_{GaAs} in the pure binary compounds.

ii) The B-As bond decreases from the GaAs value towards the BAs value and ends up only 4% higher than the value for pure BAs.

iii) The average bond length relaxation parameter[52]

$$= [R_{\mathrm{GaAs}}\ x) - R_{\mathrm{BAs}}\ x)]/[R^{0}_{\mathrm{GaAs}} - R^{0}_{\mathrm{BAs}}] \qquad 14)$$

is 0.76. ($=0$ when there is no relaxation and 1 when the relaxation is full.) Thus, assuming R_{BAs} to be Vegard-like as in the virtual crystal approximation) overestimates the bond length by $\sim 13\%$.

We also modeled a 50%-50% random alloy using a 32-atom special quasirandom structure SQS16 in Table II).[39] We found that the distribution of the bond lengths has the expected bimodal form for a random binary alloy,[53] and the B-As bonds are generally larger than the ideal B-As bond length while the Ga-As bond lengths are smaller than the ideal Ga-As bond length.

ing pure A and pure B into the in-plane lattice constant $\overline{a}$ of the superlattice, and relaxing them in the direction $\hat{G}$. ii) The interfacial energy, i.e., the difference between $\Delta H(n,\hat{G})$ and the consituent strain energy, is defined by

$$\Delta H\ n,\hat{G}) = \frac{2I\ n,\hat{G})}{n} + \Delta E_{CS}\ \overline{a},\hat{G}). \qquad 16)$$

We calculated $\Delta E_{CS}(\overline{a},\hat{G})$ for BAs and GaAs, deformed to the average lattice constant $\overline{a}$ along $\hat{G}=(001)$. This gave 148 meV/atom. From $\Delta H(n,\hat{G}=001)$ of Table V and ΔE_{CS} we calculated the interfacial energy I for $n=1$, 2, and 4. We found $I=19$, 23, and 26 meV, respectively. While a larger superlattice period n would be required to determine the converged value of I, we see that the BAs-GaAs interface is *repulsive*. This is why $\Delta H(n,\hat{G})$ of Table V *decreases* with n: larger n reduces the *proportional* effect of the interfacial repulsion.

So far we dealt with 001) superlattices. The CuPt-like monolayer $(BAs)_1/(GaAs)_1$ 111) is particularly interesting since in other Group-III–V alloys e.g., $GaInP_2$) it appears as a spontaneously ordered stucture during alloying.[59] We find a very high ΔH(CuPt) of 108 eV/atom, suggesting thermodynamic instability.

For the random alloys in Table V, all of the excess enthalpies are positive. We compare the mixing enthaplies as obtained by the LDA which includes both size-mismatched-induced strain effects and charge-transfer ''chemical'' effects) and the valence force field VFF) method which includes only strain effects)

$GaAs_{1-x}N_x$. In *epitaxial* growth experiments, the alloy solubility can dramatically exceed that in *bulk* experiments for reasons explained in Ref. 60.

D. Quasilocalized electronic states

We find that the incorporation of boron into the GaAs host material has little effect on the state at the VBM but that the lower conduction-band states are strongly peturbed. The square of the wave functions for the VBM and the lowest two conduction-band states for isolated boron in GaAs are shown in the left-hand side of Fig. 14. The first column shows the states for an isolated boron atom in the center of a supercell of GaAs. The VBM is completely delocalized and looks very much like the VBM state of pure GaAs except for a region near boron impurity where the wave function is extended towards the boron atom. This distortion is precisely what one would expect based on the strong coupling of boron *p* and arsenic *p* states at the VBM in BAs, as discussed in Secs. III B and III D. In contrast to the VBM, the CBM state shows a significant localization *around* the boron atom. The CBM shows *long-range* delocalization, but the majority of the wave function is concentrated near the boron atom. For the second lowest conduction-band state (CBM+1), the situation is similar except the wave function is concentrated around a small number of gallium atoms as well. The dual character of the conduction-band states extended at long range but concentrated around the boron atoms in the short range) indicates that the states are *resonant* in the conduction band and are not localized states *inside the gap*. The conduction-band states could be considered as boron-perturbed bulk GaAs conduction-band states.

The second column of Fig. 14 shows the same states VBM, CBM, CBM+1) for a fourth neighbor *pair* of boron atoms inside a supercell of GaAs. A statistically random distribution of boron atoms would result, among others, in pairs. In the case of $GaAs_{1-x}N_x$ alloys, the presence of nitrogen pairs can result in localized impurity states inside the gap.[61] Calculations were performed for the five symmetrically unique pair arrangements in the 64-atom supercell as described in Table III. Qualitative features of wave-function localization were the same for all of the pairs, and only the most representative case, the fourth nearest-neighbor pair, is shown in the figure. The features of the pair states are similar to those of the isolated impurity discussed above—that is, the VBM is mainly an As-derived, delocalized state while the lower CB states are concentrated around the boron atoms. Again, there is some effect on the wave function very near the boron atom. The CBM state is concentrated around the boron atom in the middle of the cell and around the boron and gallium atoms on the cell edges. The next lowest conduction-band state shows similar features and the wave function is restricted primarily to the 200) plane of the cell.

The short-range ''localization'' effects of boron incorporation into GaAs appear to be similar to those seen in $GaAs_{1-x}N_x$ alloys, resulting mainly in ''dual character'' conduction-band states that are still extended at long range but are localized around the boron atoms. However, it appears that the perturbation of boron on the near-gap states of GaAs is gentler than that of nitrogen as none of the pairs cause states inside the gap. This is another instance as with band-gap bowing and band offsets) where boron is less ''intrusive'' than its first-rowts319(ThisD (319(TeTf 9.978[(wher178[t-a5Bb)

it could be used as a relatively benign component which is added to lattice match the alloy to a given substrate.

ACKNOWLEDGMENTS

This work was supported by DOE-SC-BES-DMS under Contract No. DE-AC36-99-GO10337. We gratefully acknowledge S.-H. Wei for many helpful discussions regarding the LAPW method and a critical reading of the manuscript, and J. F. Geisz for useful discussions regarding the experimental data and techniques as well as a critical reading of the manuscript.

[1] R. Addinall, R.C. Newman, Y. Okada, and F. Orito, Semicond. Sci. Technol. **7**, 1306 1992).
[2] R. C. Newman, *Semiconductors and Semimetals* Academic, New York, 1993), Vol. 38.
[3] J. Maguire, R.C. Newman, I. Grant, D. Rumsby, and R.M. Ware, J. Phys. D **18**, 2029 1985).
[4] J. Woodhead, R.C. Newman, I. Grant, D. Rumsby, and R.M. Ware, J. Phys. C **16**, 5523 1983).
[5] G.A. Gledhill, R.C. Newman, and J. Woodhead, J. Phys. C **17**, L301 1984).
[6] S.B. Zhang and D.J. Chadi, Phys. Rev. Lett. **64**, 1789 1990).
[7] M.A. Tischler, P.M. Mooney, B.D. Parker, F. Cardone, and M.S. Goorsky, J. Appl. Phys. **71**, 984 1992).
[8] W.E. Hoke, P.J. Lemonias, D.G. Weir, and H.T. Hendricks, J. Vac. Sci. Technol. B **11**, 902 1992); S.K. Brierley, H.T. Hendricks, W.E. Hoke, P.J. Lemonias, and D.G. Weir, Appl. Phys. Lett. **63**, 812 1993).
[9] L.B. Ta, H.M. Hobgood, and R.N. Thomas, Appl. Phys. Lett. **41**, 1091 1982).
[10] S.M. Ku, J. Electrochem. Soc. **113**, 813 1966).
[11] S. Sakai, Y. Ueta, and Y. Terauchi, Jpn. J. Appl. Phys., Part 1 **32**, 4413 1993).
[12] V.G. Vorob'ev, Z.S. Medvedeva, and V.V. Sobolev, Izv. Akad. Nauk SSSR, Neorg. Mater. [Inorg. Mater. Transl. of Neorg. Mater.) **3**, 959 1967)].
[13] T.L. Chu and A.E. Hyslop, J. Appl. Phys. **43**, 276 1972); J. Electrochem. Soc. **121**, 412 1974).
[14] A.J. Perri, S. LaPlaca, and B. Post, Acta Crystallogr. **11**, 310 1958).
[15] F.V. Williams and R.A. Ruehrwein, J. Am. Chem. Soc. **82**, 1330 1960).
[16] H.M. Manasevit, W.B. Hewitt, A.J. Nelson, and A.R. Mason, J. Electrochem. Soc. **136**, 3070 1989).
[17] M. L. Timmons, Final Technical Report for *Very High Efficiency Solar Cells*, Department of Defense, Office of Contracts, Contract No. NRO-95-C-3001, 1998.
[18] J.F. Geisz, D.J. Friedman, J.M. Olson, Sarah R. Kurtz, R.C. Reedy, A.B. Swartzlander, B.M. Keyes, and A.G. Norman, Appl. Phys. Lett. **76**, 1443 2000).
[19] D.J. Stukel, Phys. Rev. B **1**, 3458 1970).
[20] R.M. Wentzcovitch and M.L. Cohen, J. Phys. C **19**, 6791 1986).
[21] R.M. Wentzcovitch, M.L. Cohen, and P.K. Lam, Phys. Rev. B **36**, 6058 1987).
[22] C. Prasad and M. Sahay, Phys. Status Solidi B **154**, 201 1989).
[23] M. Ferhat, A. Zaoui, M. Certier, and H. Aourag, Physica B **252**, 229 1998).
[24] M.P. Surh, S.G. Louie, and M.L. Cohen, Phys. Rev. B **43**, 9126 1991).
[25] F. Benkabou, C. Chikr.Z, H. Aourag, P.J. Becker, and M. Certier, Phys. Lett. A **252**, 71 1999).
[26] B. Bouhafs, H. Aourag, M. Ferhat, and M. Certier, J. Phys.: Condens. Matter **11**, 5781 1999).
[27] T. Mattila, S.-H. Wei, and A. Zunger, Phys. Rev. B **60**, R11 245 1999).
[28] L. Bellaiche, T. Mattila, S.-H. Wei, and A. Zunger, Phys. Rev. B **74**, 1842 1999).
[29] S.-H. Wei and A. Zunger, Phys. Rev. B **43**, 1662 1991); J. Appl. Phys. **78**, 3846 1995); Phys. Rev. Lett. **76**, 664 1996).
[30] P. Hohenberg and W. Kohn, Phys. Rev. B **136**, B864 1964); W. Kohn and L.J. Sham, *ibid.* **140**, A1133 1965).
[31] S.-H Wei and H. Krakauer, Phys. Rev. Lett. **55**, 1200 1985), and references therein; D. J. Singh, *Planewaves, Pseudopotential and the LAPW Method* Kluwer Academic, Boston, 1994), and references therein.
[32] D.J. Singh, Phys. Rev. B **43**, 6388 1991).
[33] P. Blaha, K. Schwarz, and J. Luitz, WIEN97, Vienna University of Technology, Vienna, 1997; Updated version of P. Blaha, K. Schwarz, P. Sorantin, and S.B. Trickey, Comput. Phys. Commun. **59**, 399 1990).
[34] J.P. Perdew and Y. Wang, Phys. Rev. B **45**, 13 244 1992).
[35] H.J. Monkhorst and J.D. Pack, Phys. Rev. B **13**, 5188 1976).
[36] S. Froyen, Phys. Rev. B **39**, 3168 1989).
[37] Tetrahedral radii are in angstroms

[46] C.S. Wang and B.M. Klein, Phys. Rev. B **24**, 3393 1981).
[47] Z.W. Lu and A. Zunger, Phys. Rev. B **47**, 9385 1993).
[48] S.-H. Wei and A. Zunger, Appl. Phys. Lett. **72**, 2011 1998).
[49] S.-H. Wei and A. Zunger, Phys. Rev. Lett. **59**, 144 1987).
[50] J.F. Geisz, D.J. Friedman, Sarah R. Kurtz, and B.M. Keyes, J. Cryst. Growth **195**, 401 1998).
[51] R. Magri, S. Froyen, and A. Zunger, Phys. Rev. B **44**, 7947 1991).
[52] J.L. Martins and A. Zunger, Phys. Rev. B **30**, 6217 1984).
[53] J.C. Mikkelsen and J.B. Boyce, Phys. Rev. Lett. **49**, 1412 1982); Phys. Rev. B **28**, 7130 1983); J.B. Boyce and J.C. Mikkelsen, *ibid.* **31**, 6903 1985).
[54] *Landolt-Bornstein: Numerical Data and Functional Relationships in Science and Technology*, edited by O. Madelung, M. Schulz, and H. Weiss Springer, Berlin, 1982), Vol. 17a.
[55] J.E. Bernard and A. Zunger, Phys. Rev. B **36**, 3199 1987).
[56] L. Bellaiche, S.-H. Wei, and A. Zunger, Phys. Rev. B **56**, 10 233 1997).
[57] J. F. Geisz private communication).
[58] R.G. Dandrea, J.E. Bernard, S.-H. Wei, and A. Zunger, Phys. Rev. Lett. **64**, 36 1990).
[59] A. Zunger and S. Mahajan, in *Handbook of Semiconductors*, 2nd ed. Elsevier, Amsterdam, 1994), Vol. 3, pp. 1399–1513.
[60] S.B. Zhang and Alex Zunger, Appl. Phys. Lett. **71**, 677 1997).
[61] X. Liu, M.-E. Pistol, L. Samuelson, S. Schwetlick, and W. Seifert, Appl. Phys. Lett. **56**, 1451 1990).